Behaviour of exponential three-point coordinates at the vertices of convex polygons

Dmitry Anisimov · Kai Hormann · Teseo Schneider

Abstract

Barycentric coordinates provide a convenient way to represent a point inside a triangle as a convex combination of the triangle's vertices and to linearly interpolate data given at these vertices. Due to their favourable properties, they are commonly applied in geometric modelling, finite element methods, computer graphics, and many other fields. In some of these applications, it is desirable to extend the concept of barycentric coordinates from triangles to polygons, and several variants of such generalized barycentric coordinates have been proposed in recent years. In this paper we focus on exponential three-point coordinates, a particular one-parameter family for convex polygons, which contains Wachspress, mean value, and discrete harmonic coordinates as special cases. We analyse the behaviour of these coordinates and show that the whole family is C^0 at the vertices of the polygon and C^1 for a wide parameter range.

Citation Info

Journal
Journal of Computational and Applied Mathematics

Volume
350, April 2019

Pages
114–129

1 Introduction

Let P be a strictly convex polygon with $n \geq 3$ vertices $v_1, \dots, v_n \in \mathbb{R}^2$ in anticlockwise order. We denote the interior of P by the open set $\Omega \subset \mathbb{R}^2$ and its closure by $\bar{\Omega}$, so that $\bar{\Omega}$ is the convex hull of the vertices.

Definition 1. A set of functions $\lambda_1, \dots, \lambda_n : \bar{\Omega} \to \mathbb{R}$ is called a set of *generalized barycentric coordinates*, if the λ_i satisfy the three properties

$$\text{1) Partition of unity:} \qquad \sum_{i=1}^{n} \lambda_i(v) = 1, \qquad v \in \bar{\Omega}, \tag{1a}$$

$$\text{2) Barycentric property:} \qquad \sum_{i=1}^{n} \lambda_i(v) v_i = v, \qquad v \in \bar{\Omega}, \tag{1b}$$

$$\text{3) Lagrange property:} \qquad \lambda_i(v_j) = \delta_{i,j}, \qquad i = 1, \dots, n, \quad j = 1, \dots, n, \tag{1c}$$

where $\delta_{i,j}$ is the Kronecker delta.

If $n = 3$, so that P is a triangle, then it was already known to Möbius [5] that the corresponding barycentric coordinates are uniquely defined by

$$\lambda_i(v) = \frac{A(v, v_{i+1}, v_{i+2})}{A(v_1, v_2, v_3)}, \qquad i = 1, 2, 3,$$

where $A(x, y, z)$ denotes the signed area of the triangle $[x, y, z]$ with vertices $x, y, z \in \mathbb{R}^2$. Note that throughout this article we consider vertex indices cyclically over $1, \dots, n$, so that $v_{n+1} = v_1$ and $v_0 = v_n$, for example.

If $n \geq 4$, then such a unique definition does not exist, but Floater et al. [3] provide a simple recipe for constructing generalized barycentric coordinates. For any given set of functions $c_1, \dots, c_n : \Omega \to \mathbb{R}$, let

$$w_i(v) = \frac{c_{i+1}(v) A_{i-1}(v) - c_i(v) B_i(v) + c_{i-1}(v) A_i(v)}{A_{i-1}(v) A_i(v)}, \qquad i = 1, \dots, n, \tag{2}$$

where $A_i(v) = A(v, v_i, v_{i+1})$ and $B_i(v) = A(v, v_{i-1}, v_{i+1})$ are the signed triangle areas shown in Figure 1. The functions $\lambda_i : \Omega \to \mathbb{R}$ with

$$\lambda_i(v) = \frac{w_i(v)}{W(v)}, \qquad i = 1, \dots, n, \tag{3}$$

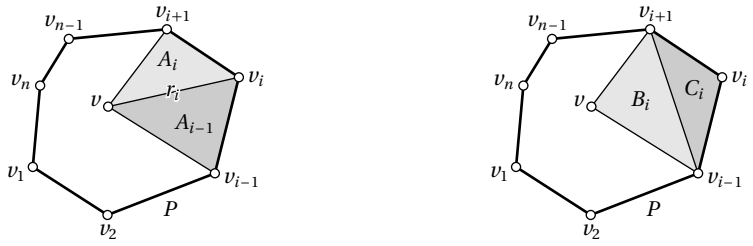

Figure 1: Notation used for the definition of exponential three-point coordinates for a planar polygon P with vertices $v_1, \dots, v_n$.

and

$$W(v) = \sum_{i=1}^{n} w_i(v), \tag{4}$$

are then well-defined and satisfy conditions (1a) and (1b) for any $v \in \Omega$, as long as the denominator $W(v)$ does not vanish. Moreover, if the w_i in (2) are non-negative on Ω, then the λ_i extend continuously to $\bar{\Omega}$ and satisfy condition (1c). However, the non-negativity of the w_i is only a sufficient condition and the recipe above usually leads to proper generalized barycentric coordinates even if it is not satisfied.

Floater et al. [3] further study the family of *exponential three-point coordinates*, which is defined by setting $c_i(v) = r_i(v)^p$ in (2) for some $p \in \mathbb{R}$ and $r_i(v) = \|v - v_i\|$ (see Figure 1). The name of this family refers to the exponent p and the fact that $w_i(v)$ in (2) depends on the three vertices v_{i-1}, v_i, v_{i+1} of P for this choice of $c_i(v)$. They realize that Wachspress coordinates [7], mean value coordinates [2], and discrete harmonic coordinates [1, 6] are special members of this family for $p = 0$, $p = 1$, and $p = 2$, respectively, and that $p = 0$ and $p = 1$ are the only choices of p for which the w_i in (2) are positive. According to the sufficient condition mentioned above, this implies that Wachspress and mean value coordinates are generalized barycentric coordinates in the sense of Definition 1, but what about other values of p?

The plots in Figures 2 and 3 suggest that exponential three-point coordinates are well-defined over $\bar{\Omega}$ for other values of p, too, and in this paper we prove that they are proper generalized barycentric coordinates for any $p \in \mathbb{R}$. To this end, let us first observe that the denominator $W(v)$ in (4) does not vanish for any $v \in \Omega$.

Proposition 1. *Exponential three-point coordinates are well-defined over Ω for any $p \in \mathbb{R}$.*

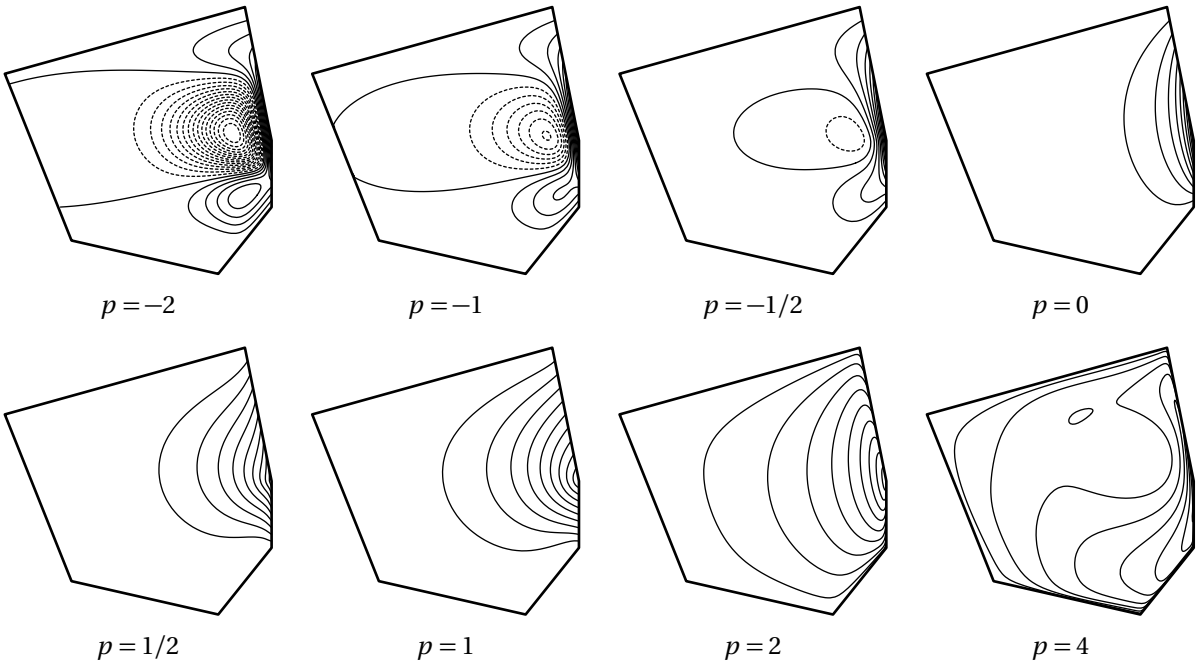

Figure 2: Contour plots for contour values $\mathbb{Z}/10$ of the exponential three-point coordinate corresponding to the middle right vertex of this convex polygon for different values of p. Dashed lines indicate negative contour values.

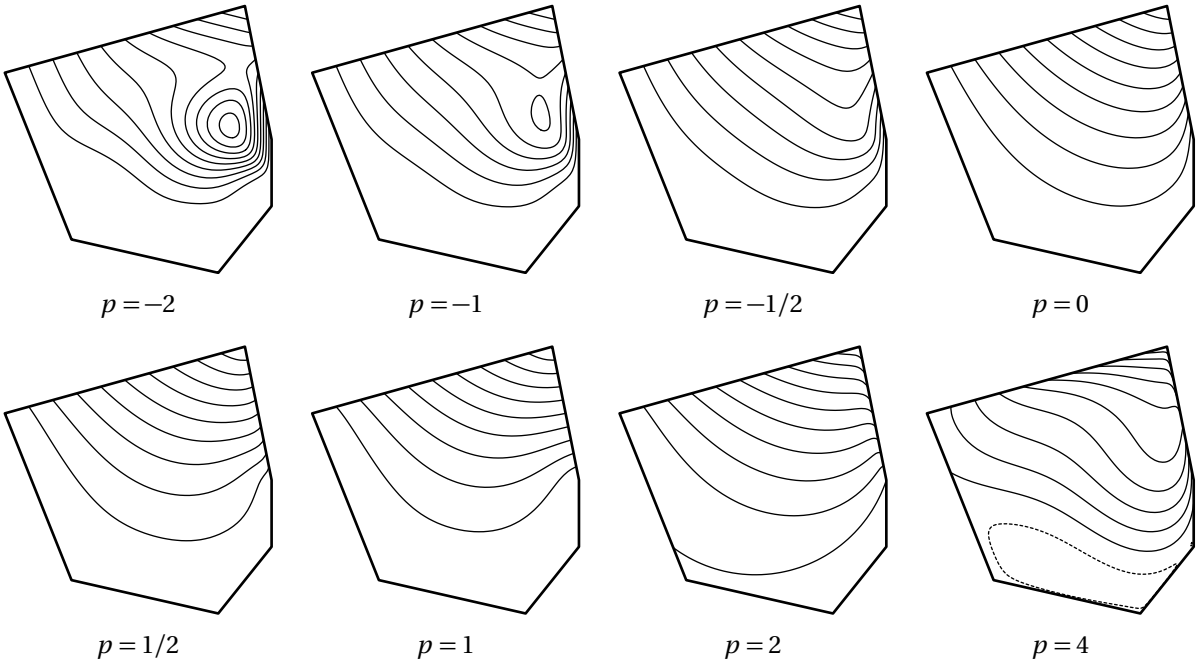

Figure 3: Contour plots for contour values $\mathbb{Z}/10$ of the exponential three-point coordinate corresponding to the top right vertex of this convex polygon for different values of p. Dashed lines indicate negative contour values.

Proof. Omitting the argument v and noticing that $A_{i-1}+A_i = B_i + C_i$ with $C_i = A(v_{i-1}, v_i, v_{i+1})$, as shown in Figure 1, we can write W as

$$\begin{aligned} W &= \sum_{i=1}^{n} \frac{r_{i+1}^p A_{i-1} - r_i^p (A_{i-1} + A_i - C_i) + r_{i-1}^p A_i}{A_{i-1} A_i} \\ &= \sum_{i=1}^{n} \frac{r_{i+1}^p - r_i^p}{A_i} + \sum_{i=1}^{n} \frac{r_i^p C_i}{A_{i-1} A_i} - \sum_{i=1}^{n} \frac{r_i^p - r_{i-1}^p}{A_{i-1}} \\ &= \sum_{i=1}^{n} \frac{r_i^p C_i}{A_{i-1} A_i}, \end{aligned} \tag{5}$$

which is clearly positive for $v \in \Omega$. Therefore, the λ_i in (3) do not have any singularities in Ω. □

Next, let us analyse the behaviour of the functions λ_i as v approaches any of the open edges $E_i = (v_i, v_{i+1})$, $i = 1, \dots, n$ of P. In this case, the area A_i converges to zero, so that w_i and w_{i+1} diverge to infinity. We can fix this problem by introducing the products

$$\mathcal{A} = \prod_{j=1}^{n} A_j, \qquad \mathcal{A}_i = \prod_{\substack{j=1 \\ j \neq i}}^{n} A_j, \qquad \mathcal{A}_{i-1,i} = \prod_{\substack{j=1 \\ j \neq i-1,i}}^{n} A_j, \qquad i = 1, \dots, n,$$

of all areas A_j and those with one or two terms missing, respectively, and considering the functions

$$\tilde{w}_i = w_i \mathcal{A} = r_{i+1}^p \mathcal{A}_i - r_i^p B_i \mathcal{A}_{i-1,i} + r_{i-1}^p \mathcal{A}_{i-1}, \qquad i = 1, \dots, n, \tag{6}$$

and

$$\tilde{W} = W \mathcal{A} = \sum_{i=1}^{n} \tilde{w}_i. \tag{7}$$

Since $\mathcal{A}$ is well-defined and does not vanish over Ω, it is clear that the functions

$$\tilde{\lambda}_i = \frac{\tilde{w}_i}{\tilde{W}}, \qquad i = 1, \dots, n, \tag{8}$$

coincide with the λ_i on Ω, but they have the advantage of being well-defined over the open edges of P.

Proposition 2. *Exponential three-point coordinates extend continuously to* $\Omega \cup E_1 \cup \cdots \cup E_n$ *and are linear along* $E_1, \ldots, E_n$ *for any* $p \in \mathbb{R}$.

Proof. Let us write $v \in E_j$ as $v = (1-t)v_j + t\,v_{j+1}$ for some $t \in (0,1)$ and note that $A_j(v) = 0$ and

$$-\frac{B_j(v)}{A_{j-1}(v)} = \frac{r_{j+1}(v)}{r_j(v)} = \frac{1-t}{t}.$$

Therefore, by (6) and omitting the argument v,

$$\tilde{w}_j = r_{j+1}^p \mathcal{A}_j + r_j^{p-1} r_{j+1} \mathcal{A}_j = \big(r_{j+1}^{p-1} + r_j^{p-1}\big) r_{j+1} \mathcal{A}_j$$

and similarly

$$\tilde{w}_{j+1} = \big(r_{j+1}^{p-1} + r_j^{p-1}\big) r_j \mathcal{A}_j.$$

Since $\tilde{w}_k = 0$ for $k \neq j, j+1$, we have

$$\tilde{W} = \tilde{w}_j + \tilde{w}_{j+1} = \big(r_{j+1}^{p-1} + r_j^{p-1}\big)\big(r_j + r_{j+1}\big)\mathcal{A}_j > 0$$

and conclude that the $\tilde{\lambda}_i$ are well-defined over E_j. Moreover,

$$\tilde{\lambda}_j = \frac{r_{j+1}}{r_j + r_{j+1}} = 1 - t, \qquad \tilde{\lambda}_{j+1} = \frac{r_j}{r_j + r_{j+1}} = t, \tag{9}$$

and $\tilde{\lambda}_k = 0$ for $k \neq j, j+1$. □

A similar trick can be used to show that the λ_i also extend continuously to the vertices v_j of P and satisfy the Lagrange property (1c), but it requires a more refined and careful analysis (Section 2). We further investigate the behaviour of the derivatives of exponential three-point coordinates at the vertices and show that they are at least C^1 for any $p < 1$ (Section 3).

2 Continuity at the vertices

The functions $\tilde{\lambda}_i$ in (8) are not well-defined at the vertices of P, except for $p = 0$, but the linear behaviour along the edges E_j in (9) implies that $\tilde{\lambda}_i(v)$ converges to $\delta_{i,j}$ as v approaches v_j along the boundary of P. It turns out that this behaviour also holds for v approaching v_j arbitrarily inside P (Section 2.1), so that a continuous extension of exponential three-point coordinates to $\bar{\Omega}$ is obtained by enforcing the Lagrange property (1c). For $p \leq 1$, the coordinates can further be extended to some region around P, but they have unremovable singularities arbitrarily close to the vertices for $p > 1$ (Section 2.2).

2.1 Convergence from inside

Let us first consider the case $p < 0$ and analyse the behaviour of the functions $\tilde{\lambda}_i$ as v approaches some vertex v_j of P. In this case, the distance r_j converges to zero, so that r_j^p and at least $\tilde{w}_j$ diverge to infinity. Similar to above, we can fix this problem by introducing the products

$$\mathcal{R} = \prod_{j=1}^{n} r_j^{-p}, \qquad \mathcal{R}_i = \prod_{\substack{j=1 \\ j \neq i}}^{n} r_j^{-p}, \qquad i = 1, \ldots, n,$$

and considering the functions

$$\hat{w}_i = \tilde{w}_i \mathcal{R} = \mathcal{R}_{i+1} \mathcal{A}_i - \mathcal{R}_i B_i \mathcal{A}_{i-1,i} + \mathcal{R}_{i-1} \mathcal{A}_{i-1}, \qquad i = 1, \ldots, n, \tag{10}$$

and

$$\hat{W} = \tilde{W} \mathcal{R} = \sum_{i=1}^{n} \hat{w}_i.$$

Since $\mathcal{R}$ is well-defined and does not vanish over $\Omega \cup E_1 \cup \cdots \cup E_n$, it is clear that the functions

$$\hat{\lambda}_i = \frac{\hat{w}_i}{\hat{W}}, \qquad i = 1, \ldots, n,$$

coincide with the $\tilde{\lambda}_i$ on $\Omega \cup E_1 \cup \cdots \cup E_n$, but they have the advantage of being well-defined at the vertices of P.

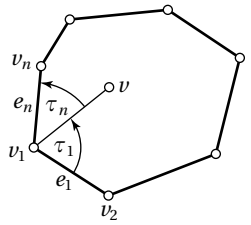

Figure 4: Notation used in the proofs of Lemmas 2 and 3.

Lemma 1. *Exponential three-point coordinates extend continuously to $\bar{\Omega}$ for $p < 0$.*

Proof. First observe that $A_{j-1}(v)$, $A_j(v)$, and $r_j(v)$ vanish at $v = v_j$. Therefore, $\mathcal{A}_i = 0$ for all i, $\mathcal{A}_{i-1,i} = \mathcal{R}_i = 0$ for $i \neq j$, and $\mathcal{A}_{j-1,j}, \mathcal{R}_j > 0$, so that all terms of the $\hat{w}_i$ in (10) vanish, except for the second term of $\hat{w}_j$. Consequently, $\hat{w}_i = 0$ for $i \neq j$, $\hat{w}_j = -\mathcal{R}_j B_j \mathcal{A}_{j-1,j} > 0$, $\hat{W} = \hat{w}_j > 0$, and finally $\hat{\lambda}_i(v_j) = \delta_{i,j}$. □

The reasoning in the proof of Lemma 1 does not carry over to the case $p > 0$, because $\mathcal{R}$ and $\mathcal{R}_i$ for $i \neq j$ diverge to infinity as v approaches v_j. However, for $0 < p < 1$, this divergence is counterbalanced by the zero-convergence of the areas A_{j-1} and A_j, so that the $\hat{w}_i$ converge to finite values at $v = v_j$.

Lemma 2. *Exponential three-point coordinates extend continuously to $\bar{\Omega}$ for $0 < p < 1$.*

Proof. Without loss of generality, we consider the case where v approaches v_1, so that A_1, A_n, and r_1 converge to zero, while all other A_i and r_i converge to positive real numbers. The key idea now is to show that the two quotients A_1/r_1^p and A_n/r_1^p converge to zero, too. Denoting the length of E_1 by $e_1 = \|v_2 - v_1\|$ and the signed angle between the vectors $v_2 - v_1$ and $v - v_1$ by τ_1 (see Figure 4), we can bound the first quotient as

$$0 \leq \frac{A_1}{r_1^p} = \frac{r_1 e_1 \sin \tau_1}{2 r_1^p} \leq \frac{r_1^{1-p} e_1}{2} \tag{11}$$

for any $v \in \Omega$. Since the upper bound is zero at $v = v_1$, we conclude

$$\lim_{v \to v_1} \frac{A_1(v)}{r_1(v)^p} = 0 \tag{12}$$

and similarly

$$\lim_{v \to v_1} \frac{A_n(v)}{r_1(v)^p} = 0. \tag{13}$$

It follows that all terms of the $\hat{w}_i$ in (10) with a diverging factor $\mathcal{R}_i$, $i \neq 1$, converge to zero, because they contain one of these two quotients. Among the other three terms with factor $\mathcal{R}_1$, which is finite at $v = v_1$, the terms in $\hat{w}_2$ and $\hat{w}_n$ are zero, because $\mathcal{A}_1$ and $\mathcal{A}_n$ vanish, so that only the second term in $\hat{w}_1$ is non-zero. Consequently, $\lim_{v \to v_1} \hat{w}_i(v) = 0$ for $i \neq 1$, $\lim_{v \to v_1} \hat{w}_1(v) = -\mathcal{R}_1(v_1) B_1(v_1) \mathcal{A}_{n,1}(v_1) > 0$, $\lim_{v \to v_1} \hat{W}(v) = \lim_{v \to v_1} \hat{w}_1(v)$, and therefore $\lim_{v \to v_1} \hat{\lambda}_i(v) = \delta_{i,1}$. □

The proof of Lemma 2 does not extend to the case $p > 1$, because the upper bound in (11) diverges. Going back to the functions $\tilde{\lambda}_i$ in (8), we see that they are not well-defined at the vertices of P, because all the $\tilde{w}_i$ and thus also $\tilde{W}$ are zero at $v = v_j$. However, for $p > 1$, this problem can be fixed by considering the functions $\tilde{w}_i / r_j$, $i = 1, \ldots, n$, and $\tilde{W}/r_j$.

Lemma 3. *Exponential three-point coordinates extend continuously to $\bar{\Omega}$ for $p > 1$.*

Proof. As in the proof of Lemma 2, we consider only the case where v approaches v_1. Like in (11), we can bound the quotients A_1/r_1 and A_n/r_1 for any $v \in \Omega$ as

$$0 \leq \frac{A_1}{r_1} \leq \frac{e_1}{2}, \qquad 0 \leq \frac{A_n}{r_1} \leq \frac{e_n}{2}, \tag{14}$$

where $e_n = \|v_n - v_1\|$ is the length of E_n (see Figure 4). Since these bounds are constants, they also hold in the limit. For $i \neq 1$, we then observe that all terms of $\tilde{w}_i$ in (6) contain either A_1 or A_n plus one other factor (A_1, A_n, B_2, B_n, or r_1^p) that vanishes at v_1, so that $\lim_{v \to v_1} \tilde{w}_i(v)/r_1(v) = 0$. It remains to show that

$$\frac{\tilde{w}_1}{r_1} = \left(\frac{r_2^p A_n}{r_1} - r_1^{p-1} B_1 + \frac{r_n^p A_1}{r_1} \right) \mathcal{A}_{n,1},$$

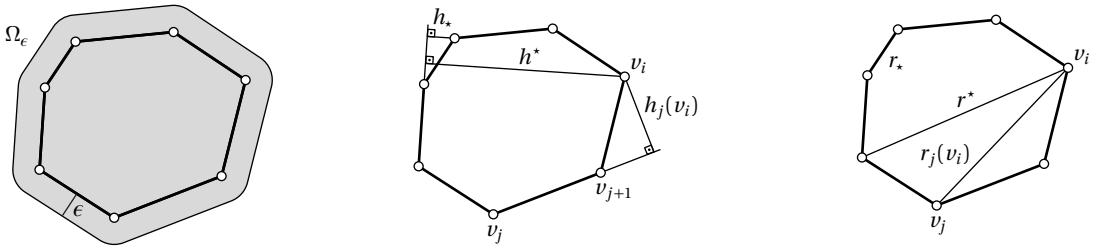

Figure 5: Notation used in Section 2.2.

and thus also $\tilde{W}/r_1$, converges to a non-zero, finite value. By (14),

$$\frac{r_2^p A_n}{r_1} + \frac{r_n^p A_1}{r_1} \leq \frac{r_2^p e_n + r_n^p e_1}{2}$$

for any $v \in \Omega$ and this upper bound converges to the positive constant $c^\star = (e_1^p e_n + e_n^p e_1)/2$. Moreover,

$$\begin{aligned}\frac{r_2^p A_n}{r_1} + \frac{r_n^p A_1}{r_1} &= \frac{r_2^p e_n \sin\tau_n + r_n^p e_1 \sin\tau_1}{2} \\ &\geq \min(r_2, r_n)^p \min(e_1, e_n)(\sin\tau_1 + \sin\tau_n)/2 \\ &\geq \min(r_2, r_n)^p \min(e_1, e_n)(\sin\tau_1 \cos\tau_n + \sin\tau_n \cos\tau_1)/2 \\ &= \min(r_2, r_n)^p \min(e_1, e_n)\sin(\tau_1 + \tau_n)/2,\end{aligned}$$

where τ_n is the signed angle between $v - v_1$ and $v_n - v_1$ (see Figure 4), and this lower bound converges to the positive constant $c_\star = \min(e_1, e_n)^{p+1} \sin(\tau_1 + \tau_n)/2$. It follows that $(r_2^p A_n + r_n^p A_1)/r_1$ converges to a positive, finite value $c \in [c_\star, c^\star]$ and since r_1^{p-1} vanishes at $v = v_1$ and $\mathcal{A}_{n,1}$ does not, the proof is complete. Note that the limit $c\,\mathcal{A}_{n-1}$ of $\tilde{w}_1/r_1$ may not be the same for two different sequences of v, which both converge to v_1, but this does not affect the proof, because the ratio $(\tilde{w}_1/r_1)/(\tilde{W}/r_1)$ always converges to 1. □

We are now ready to summarize our observations.

Theorem 1. *Exponential three-point coordinates are continuous generalized barycentric coordinates over* $\bar{\Omega}$ *for any* $p \in \mathbb{R}$.

Proof. It follows from Proposition 1 and Proposition 5 in [3] that exponential three-point coordinates are continuous and satisfy conditions (1a) and (1b) over Ω for any $p \in \mathbb{R}$. Proposition 2 and Lemmas 1, 2, and 3 further show that they can be extended continuously to $\bar{\Omega}$ for $p \notin \{0, 1\}$ and that this extension satisfies condition (1c) and is piecewise linear along the boundary of P. For $p = 0$ and $p = 1$, the same boundary behaviour follows from Corollary 2 in [3], and it implies that conditions (1a) and (1b) hold for any point on the boundary of P and thus for any $v \in \bar{\Omega}$. □

2.2 Convergence from outside

Let us now enlarge the domain from $\bar{\Omega}$ to the open set Ω_ϵ by adding all points $v \in \mathbb{R}^2$, which are ϵ-close to Ω (see Figure 5), and analyse the continuity of exponential three-point coordinates over Ω_ϵ.

To this end, let $h_j(v)$ be the (shortest) distance between a point v and the line through v_j and v_{j+1}, and let

$$h_\star = \min_{\substack{i,j=1,\dots,n \\ j \neq i-1,i}} h_j(v_i), \qquad h^\star = \max_{i,j=1,\dots,n} h_j(v_i)$$

be the minimum and maximum distance between the vertices and the supporting lines of P. We further denote the minima and maxima of distances between vertices of P, of edge lengths, and of areas C_i by

$$\begin{aligned} r_\star &= \min_{\substack{i,j=1,\dots,n \\ j \neq i}} r_j(v_i), & r^\star &= \max_{i,j=1,\dots,n} r_j(v_i), \\ e_\star &= \min_{i=1,\dots,n} \|v_i - v_{i+1}\|, & e^\star &= \max_{i=1,\dots,n} \|v_i - v_{i+1}\|, \\ C_\star &= \min_{i=1,\dots,n} C_i, & C^\star &= \max_{i=1,\dots,n} C_i, \end{aligned}$$

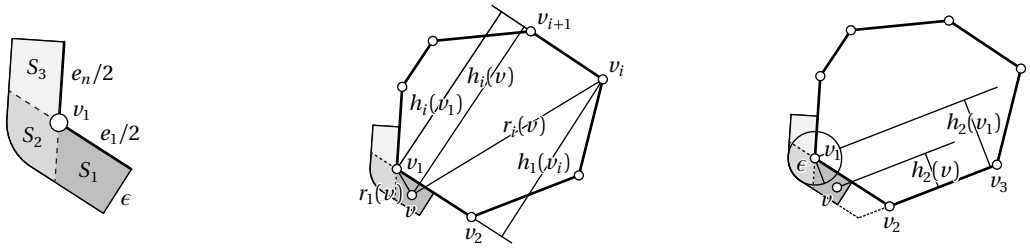

Figure 6: Notation used in the proofs of Lemmas 4 and 5.

respectively and finally introduce the positive constants

$$c_\star = \min(h_\star, r_\star, e_\star, C_\star), \qquad c^\star = \min(h^\star, r^\star, e^\star, C^\star), \tag{15}$$

which we use for defining upper bounds on ϵ that guarantee $\tilde{W}$ to be positive over $\Omega_\epsilon \setminus \bar{\Omega}$ for $p < 1$.

Lemma 4. *If $p < 0$ and*

$$\epsilon < \frac{c_\star}{n 8^n} \left(\frac{c_\star}{c^\star} \right)^{2n-p}, \tag{16}$$

then $\tilde{W}(v) > 0$ for any $v \in \Omega_\epsilon \setminus \bar{\Omega}$.

Proof. Since $n \geq 3$, $p < 0$, and $c_\star \leq c^\star$, we conclude from (16) that

$$\epsilon < c_\star/4. \tag{17}$$

Without loss of generality, we now focus on the situation around v_1 and consider the three regions (see Figure 6)

$$\begin{aligned} S_1 &= \big\{ v \in \Omega_\epsilon : A_1(v) < 0, A_n(v) \geq 0, r_1(v) \leq r_2(v) \big\}, \\ S_2 &= \big\{ v \in \Omega_\epsilon : A_1(v) < 0, A_n(v) < 0 \big\}, \\ S_3 &= \big\{ v \in \Omega_\epsilon : A_1(v) \geq 0, A_n(v) < 0, r_1(v) \leq r_n(v) \big\}, \end{aligned} \tag{18}$$

because all other cases follow by symmetry.

Let us start with the case $v \in S_1$ and establish some bounds for $r_i(v)$ and $A_i(v)$. Since v is closer to v_1 than to v_2, we can use the triangle inequality and (17) to get

$$r_1(v) \leq e_1/2 + \epsilon < e^\star/2 + c_\star/4 < c^\star$$

and thus

$$r_1^p > (c^\star)^p, \tag{19}$$

because $p < 0$. Moreover, since v and v_i for $i \geq 3$ lie on opposite sides of the line through v_1 and v_2, we have

$$r_i(v) > h_1(v_i) \geq h_\star \geq c_\star, \qquad i = 3, \ldots, n. \tag{20}$$

We next derive some bounds for $h_i(v)$, which then turn into bounds for $A_i(v)$ because $|A_i(v)| = e_i h_i(v)/2$. We first note that $h_1(v) < \epsilon$, hence

$$|A_1(v)| = e_1 h_1(v)/2 < e^\star \epsilon \leq c^\star \epsilon. \tag{21}$$

In general, we can get an upper bound for all $h_i(v)$ by triangle inequality,

$$h_i(v) \leq h_i(v_1) + r_1(v) < h^\star + c^\star \leq 2c^\star.$$

For $i = 2$, a lower bound can be obtained by recalling that v is closer to v_1 than to v_2, so that

$$h_2(v) > h_2(v_1)/2 - \epsilon > h_\star/2 - c_\star/4 \geq c_\star/4.$$

For $i \geq 3$, the minimum distance from any point on the edge $[v_1, v_2]$ to the line through v_i and v_{i+1} is either $h_i(v_1)$ or $h_i(v_2)$, and so, since v is ϵ-close to $[v_1, v_2]$,

$$h_i(v) > \min(h_i(v_1), h_i(v_2)) - \epsilon > h_\star - c_\star/4 > c_\star/4.$$

Overall, we conclude that

$$\frac{(c_\star)^2}{8} < A_i(v) < (c^\star)^2, \qquad i = 2, \dots, n. \tag{22}$$

The idea now is to use (5) to rewrite $\tilde{W}$ in (7) as

$$\tilde{W} = r_1^p C_1 \mathcal{A}_{n,1} + r_2^p C_2 \mathcal{A}_{1,2} - |A_1| \sum_{i=3}^{n} r_i^p C_i \mathcal{A}_{1,i-1,i} \tag{23}$$

with

$$\mathcal{A}_{1,i-1,i} = \prod_{\substack{j=2 \\ j \neq i-1,i}}^{n} A_j, \qquad i = 3, \dots, n,$$

and to show that the first term in (23) dominates the last term. To this end, we observe that

$$\begin{aligned}
\frac{(c^\star)^p C_1 \mathcal{A}_{n,1}}{c^\star \sum_{i=3}^n r_i^p C_i \mathcal{A}_{1,i-1,i}} &\overset{(15)}{\geq} \frac{(c^\star)^p c_\star \mathcal{A}_{n,1}}{c^\star \sum_{i=3}^n r_i^p c^\star \mathcal{A}_{1,i-1,i}} \\
&\overset{(20)}{>} \frac{(c^\star)^p c_\star \mathcal{A}_{n,1}}{c^\star \sum_{i=3}^n (c_\star)^p c^\star \mathcal{A}_{1,i-1,i}} \\
&\overset{(22)}{>} \frac{(c^\star)^p c_\star (c_\star)^{2(n-2)}/8^{n-2}}{c^\star \sum_{i=3}^n (c_\star)^p c^\star (c^\star)^{2(n-3)}} = \frac{(c_\star)^{2n-3-p}}{(n-2)8^{n-2}(c^\star)^{2n-4-p}} \\
&\overset{(16)}{>} 2\epsilon,
\end{aligned}$$

where we obtain the second inequality by recalling that $p < 0$, and so

$$\frac{1}{2}(c^\star)^p C_1 \mathcal{A}_{n,1} > c^\star \epsilon \sum_{i=3}^{n} r_i^p C_i \mathcal{A}_{1,i-1,i}.$$

Using (19) and (21), we then conclude

$$\frac{1}{2} r_1^p C_1 \mathcal{A}_{n,1} > |A_1| \sum_{i=3}^{n} r_i^p C_i \mathcal{A}_{1,i-1,i}, \tag{24}$$

which implies $\tilde{W} > 0$, and similar arguments lead to

$$\frac{1}{2} r_1^p C_1 \mathcal{A}_{n,1} > |A_n| \sum_{i=2}^{n-1} r_i^p C_i \mathcal{A}_{n,i-1,i} \tag{25}$$

for the case $v \in S_3$.

If $v \in S_2$, then we rewrite $\tilde{W}$ as

$$\tilde{W} = r_1^p C_1 \mathcal{A}_{n,1} - |A_1| r_n^p C_n \mathcal{A}_{1,n-1,n} - |A_n| r_2^p C_2 \mathcal{A}_{n,1,2} + \sum_{i=3}^{n-1} r_i^p C_i \mathcal{A}_{i-1,i},$$

which is positive because of (24) and (25), which are also valid in this case. □

Lemma 5. *If* $0 \leq p < 1$ *and*

$$\epsilon < c_\star \left(\frac{1}{n 8^n} \left(\frac{c_\star}{c^\star} \right)^{2n} \right)^{\frac{1}{1-p}}, \tag{26}$$

then $\tilde{W}(v) > 0$ *for any* $v \in \Omega_\epsilon \setminus \bar{\Omega}$.

Proof. As in the proof of Lemma 4, it follows from (26) that $\epsilon < c_\star/4$, and we proceed by considering the first of the three regions in (18). For any $v \in S_1$, the bounds in (21) and (22) still hold, and we further observe that

$$|A_1(v)| = e_1 h_1(v)/2 \leq e^\star r_1(v)/2 < c^\star r_1(v)$$

and therefore

$$r_1^p \geq (|A_1|/c^\star)^p. \tag{27}$$

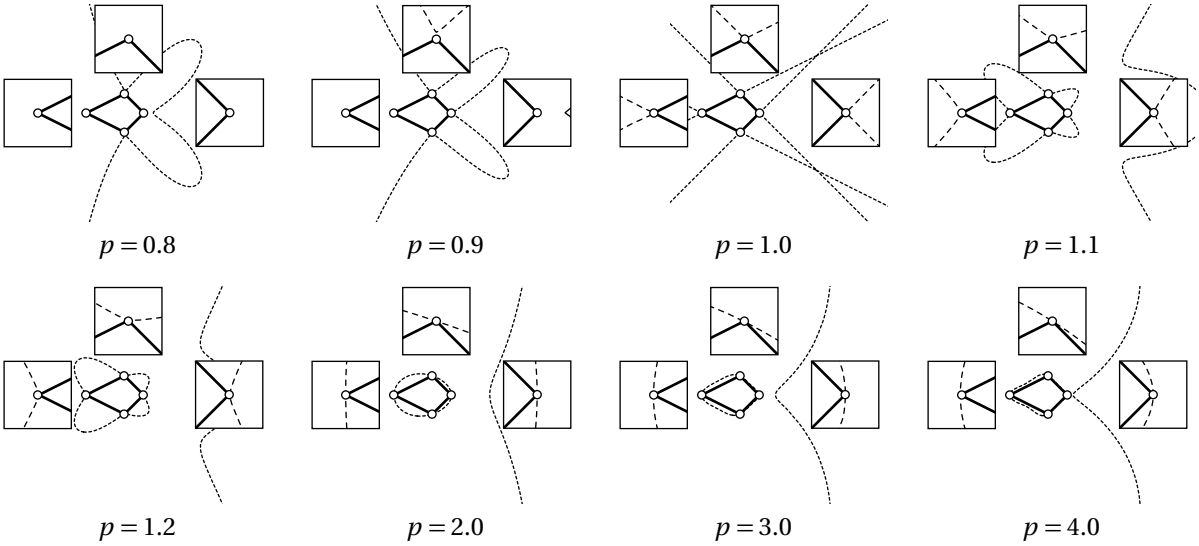

Figure 7: Plots of the zero level curve $\{v \in \mathbb{R}^2 : \tilde{W}(v) = 0\}$ for a convex polygon with four vertices and different values of p. The close-ups to the vertices of the polygon use a magnification factor of 30.

Moreover, by triangle inequality we get the upper bound

$$r_i(v) \le r_1(v) + r_i(v_1) < e_1/2 + \epsilon + r_i(v_1) < c^\star/2 + c^\star/4 + c^\star < 2c^\star \tag{28}$$

for any i. With these bounds at hand we conclude that

$$\begin{aligned}
\frac{C_1\mathcal{A}_{n,1}}{(c^\star)^p \sum_{i=3}^n r_i^p C_i \mathcal{A}_{1,i-1,i}} &\overset{(15)}{\ge} \frac{c_\star \mathcal{A}_{n,1}}{(c^\star)^p \sum_{i=3}^n r_i^p c^\star \mathcal{A}_{1,i-1,i}} \\
&\overset{(28)}{\ge} \frac{c_\star \mathcal{A}_{n,1}}{(c^\star)^p \sum_{i=3}^n (2c^\star)^p c^\star \mathcal{A}_{1,i-1,i}} \\
&\overset{(22)}{>} \frac{c_\star (c_\star)^{2(n-2)}/8^{n-2}}{(c^\star)^p \sum_{i=3}^n (2c^\star)^p c^\star (c^\star)^{2(n-3)}} = \frac{(c^\star)^{2(1-p)}}{2^p (n-2) 8^{n-2}} \left(\frac{c_\star}{c^\star}\right)^{2n-3} \\
&> 2(c^\star)^{1-p} (c_\star)^{1-p} \frac{1}{n8^n} \left(\frac{c_\star}{c^\star}\right)^{2n} \\
&\overset{(26)}{>} 2(c^\star \epsilon)^{1-p} \\
&\overset{(21)}{>} 2|A_1|^{1-p},
\end{aligned}$$

so that

$$\frac{1}{2}(|A_1|/c^\star)^p C_1 \mathcal{A}_{n,1} > |A_1| \sum_{i=3}^n r_i^p C_i \mathcal{A}_{1,i-1,i}.$$

Using (27), we then get

$$\frac{1}{2} r_1^p C_1 \mathcal{A}_{n,1} > |A_1| \sum_{i=3}^n r_i^p C_i \mathcal{A}_{1,i-1,i},$$

which implies $\tilde{W} > 0$, exactly as in the proof of Lemma 4, and also the other cases $v \in S_3$ and $v \in S_2$ follow analogously. □

The reasoning in Lemma 5 does not extend to the case $p = 1$, because the upper bound in (26) converges to 0 as p approaches 1. This suggests that $\tilde{W}$ vanishes at the vertices of P for $p \ge 1$, and Figure 7 confirms that the zero level curve $\{v \in \mathbb{R}^2 : \tilde{W}(v) = 0\}$ passes through the vertices of P for $p \ge 1$. For $p = 1$, this is not a problem, and Hormann and Floater [4] prove that the corresponding mean value coordinates are continuous over $\mathbb{R}^2$. But the following two examples show that exponential three-point coordinates for $p > 1$ can have non-removable singularities in $\mathbb{R}^2 \setminus \bar{\Omega}$ arbitrarily close to the vertices of P, and so they are, in general, not continuous over Ω_ϵ for any $\epsilon > 0$. Note that the polygons in both examples were chosen to keep

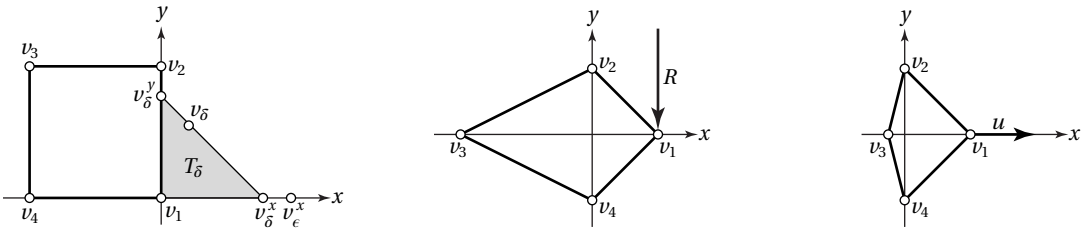

Figure 8: Notation used in Examples 1, 2, and 3.

the calculations as simple as possible, but we observed the same phenomena for all other polygons that we tested.

Example 1. Let us examine the exponential three-point coordinates for $1 < p < 2$ over the unit square P with vertices $v_1 = (0,0)$, $v_2 = (0,1)$, $v_3 = (-1,1)$, $v_4 = (-1,0)$ (see Figure 8, left). For $x \geq 0$, it turns out that

$$\tilde{W}(x,0) = (x^p(1+x) - (1+x)^p x)/8,$$

hence $\tilde{W}(0,0) = 0$ and $(\partial \tilde{W}/\partial x)(0,0) = -1/8$, because $p > 1$. Consequently, there exists some $\epsilon \in (0,1)$, such that $\tilde{W}$ is negative over the open edge between $v_1 = (0,0)$ and $v_\epsilon^x = (\epsilon, 0)$, and from Proposition 2 we know that $\tilde{W}$ is positive over the open edge between v_1 and $v_\epsilon^y = (0,\epsilon)$. It follows that for any $\delta \in (0,\epsilon)$ there exists some point v_δ on the open edge (v_δ^x, v_δ^y), such that $\tilde{W}(v_\delta) = 0$.

At least for the coordinate function $\lambda_3 = \tilde{w}_3/\tilde{W}$ it is easy to see that these singularities are non-removable close to v_1, because $\tilde{w}_3$ is negative over the open triangle $T_\delta = (v_1, v_\delta^x, v_\delta^y)$ for δ sufficiently small. To see this, we recall from (6) that $\tilde{w}_3 = \bar{w}_3 A_1 A_4$ with

$$\bar{w}_3(v) = r_4(v)^p A_2(v) - r_3(v)^p B_3(v) + r_2(v)^p A_3(v).$$

Since $\bar{w}_3(v_1) = 1 - 2^{\frac{p}{2}-1} > 0$ for $p < 2$, there exists some $\delta > 0$ such that $\bar{w}_3$ is positive over T_δ. Therefore, $\tilde{w}_3$ is negative over T_δ, because A_1 is negative and A_4 is positive over this region.

Despite the existence of these non-removable singularities, it seems hard to find an example of a sequence $(u_k)_{k\in\mathbb{N}}$ with $\lim_{k\to\infty} u_k = v_j$, such that $\lim_{k\to\infty} \lambda_i(u_k) \neq \lambda_i(v_j)$ in the case $1 < p < 2$. In particular, our numerical experiments suggest that λ_i always converges to the correct value at v_j, if v_j is approached along any line through v_j. This is not the case for $p \geq 2$, though.

Example 2. For the case $p \geq 2$, we consider the quadrilateral P with vertices $v_1 = (1,0)$, $v_2 = (0,1)$, $v_3 = (-2,0)$, $v_4 = (0,-1)$ and study the behaviour of λ_1 along the vertical ray $R = \{(1,y) : y > 0\}$ (see Figure 8, middle). For $p = 2$, we find that $\lambda_1(1,y) = (9 - 4y^2)/15$ for $y > 0$, hence

$$\lim_{\substack{v\to v_1 \\ v\in R}} \lambda_1(v) = \lim_{y\to 0^+} \lambda_1(1,y) = 3/5 < 1 = \lambda_1(v_1),$$

which shows that λ_1 is not continuous over Ω_ϵ for any $\epsilon > 0$. For $p > 2$, we get

$$w_1(1,y) = 2\frac{(1+(1+y)^2)^{\frac{p}{2}} - (1+(1-y)^2)^{\frac{p}{2}}}{y} - 4y^{p-2}$$

for $y > 0$, and using L'Hôpital's rule, we obtain

$$\lim_{y\to 0^+} w_1(1,y) = 2^{\frac{p}{2}+1} p.$$

Similar reasoning shows that

$$\lim_{y\to 0^+} W(1,y) = 2^{\frac{p}{2}+1} p + 8(3^{p-1} - 2^{\frac{p}{2}})/3,$$

hence

$$\lim_{\substack{v\to v_1 \\ v\in R}} \lambda_1(v) = \lim_{y\to 0^+} \frac{w_1(1,y)}{W(1,y)} = \frac{9p}{9p + 3^p 2^{2-\frac{p}{2}} - 12} < 1 = \lambda_1(v_1),$$

which again demonstrates that λ_1 is not continuous over Ω_ϵ for any $\epsilon > 0$.

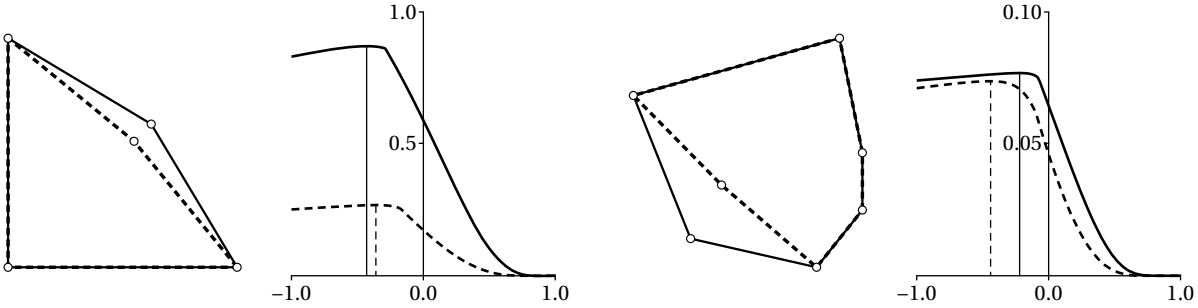

Figure 9: Plots of maximal ϵ over $p \in [-1,1)$, such that the exponential three-point coordinates are well-defined over the enlarged region Ω_ϵ for four different convex polygons (solid and dashed lines) with common bounding box $[-1,1]^2$. The vertical lines in the plots indicate the values of p that correspond to the largest maximal ϵ and hence allow for the biggest enlargement of Ω.

We should point out that the direction of the ray R does not by chance happen to be tangent to the zero level curve $\{v \in \mathbb{R}^2 : \tilde{W}(v) = 0\}$ at v_1 in this example. In fact, our numerical experiments suggest that λ_i converges to the correct value at v_j along any other line through v_j.

Let us conclude this section by summarizing our observations.

Theorem 2. *For any $p \leq 1$, there exists an $\epsilon > 0$, such that the exponential three-point coordinates are continuous generalized barycentric coordinates over Ω_ϵ.*

Proof. For $p = 1$, the statement is proven in [4], and for $p < 1$, it follows from Theorem 1, Lemmas 4 and 5, and by noting that Lemmas 1 and 2 carry over from $\bar{\Omega}$ to Ω_ϵ. The proof of Lemma 1 extends because $\hat{W}(v) > 0$ for any $v \in \Omega_\epsilon$, and the only change in the proof of Lemma 2 is that the lower bound for the quotient A_1/r_1^p in (11) must be replaced by $-r_1^{1-p} e_1/2$, because A_1 can now be negative, but this does not affect the limit in (12) and similarly for the limit in (13). □

While the upper bounds on ϵ in Lemmas 4 and 5 are very small and of theoretical interest only, exponential three-point coordinates are well-defined over Ω_ϵ for much larger values of ϵ in practice. Figure 9 reports the numerically determined maximal values of ϵ for some examples and $-1 \leq p < 1$. For the first polygon with vertices $v_1 = (-1,-1)$, $v_2 = (1,-1)$, $v_3 = (1/4,1/4)$, $v_4 = (-1,1)$, the domain Ω can be enlarged by about half the shortest edge length, as long as p is negative, with the maximum value of $\epsilon \approx 0.87$ occurring at $p \approx -0.43$. For positive p, the maximal ϵ decreases monotonically to values below 0.01 for $p \geq 0.72$. Replacing v_3 with $v_3 = (1/10,1/10)$, as indicated by the dashed lines, does not change this behaviour, but scales the values by about $1/3$, and they converge to 0 for all $p < 1$, as the exterior angle at v_3 converges to zero. The small exterior angle at the middle right vertex of the second polygon with six vertices (cf. Figures 2 and 3) is also the reason why the values of the maximal ϵ are smaller in this example, but the overall shape of the plot is similar, with the maximal value of $\epsilon \approx 0.077$ occurring at $p \approx -0.22$. Note how the position of the maximum changes as the exterior angle of the bottom left vertex becomes the dominating smallest exterior angle.

3 Differentiability at the vertices

Since exponential three-point coordinates are continuous over Ω_ϵ, and in particular in an ϵ-neighbourhood of the vertices v_j for $p \leq 1$, it seems natural to further study the differentiability at v_j. Wachspress coordinates ($p = 0$) are rational functions and therefore infinitely differentiable over Ω_ϵ and in particular at v_j. Mean value coordinates ($p = 1$) instead have been shown [4] to be C^∞ for any $v \in \mathbb{R}^2$, except at the vertices v_j, where they are only C^0. However, it turns out that the case $p = 1$ is very special (Section 3.1) and that three-point coordinates are at least C^1 at v_j for any $p < 1$.

To carry out this analysis, let us remember the notion of the directional derivative

$$\nabla_u \hat{\lambda}_i(v_j) = \lim_{h \to 0} \frac{\hat{\lambda}_i(v_j + h\,u) - \hat{\lambda}_i(v_j)}{h}$$

of $\hat{\lambda}_i$ at v_j in direction $u \in \mathbb{R}^2$, and that a necessary condition for the differentiability of $\hat{\lambda}_i$ at v_j is the

existence of a gradient $\nabla\hat{\lambda}_i(v_j)$, which satisfies

$$\nabla_u\hat{\lambda}_i(v_j)=\nabla\hat{\lambda}_i(v_j)\cdot u. \tag{29}$$

Because of the linear behaviour of exponential three-point coordinates along the edges P, as shown in Proposition 2, it is clear that the directional derivative along the adjacent edges E_{j-1} and E_j, that is, in the directions $u^-=v_{j-1}-v_j$ and $u^+=v_{j+1}-v_j$, is

$$\nabla_{u^-}\hat{\lambda}_i(v_j)=\begin{cases}1, & i=j-1,\\ -1, & i=j,\\ 0, & \text{otherwise,}\end{cases}\qquad\text{and}\qquad \nabla_{u^+}\hat{\lambda}_i(v_j)=\begin{cases}-1, & i=j,\\ 1, & i=j+1,\\ 0, & \text{otherwise,}\end{cases} \tag{30}$$

respectively. Some simple algebra then shows that the only choice of $\nabla\hat{\lambda}_i(v_j)$ that satisfies (29) for $u=u^+$ and $u=u^-$, is

$$\nabla\hat{\lambda}_i(v_j)=\frac{1}{C_j}\begin{cases}\nabla A_j, & i=j-1,\\ -\nabla B_j, & i=j,\\ \nabla A_{j-1}, & i=j+1,\\ 0, & \text{otherwise,}\end{cases} \tag{31}$$

and this choice is indeed the limit of $\nabla\hat{\lambda}_i(v)$ as v approaches v_j.

Lemma 6. *If $p<1$, then*

$$\lim_{v\to v_j}\nabla\hat{\lambda}_i(v)=\nabla\hat{\lambda}_i(v_j),\qquad i=1,\dots,n,\quad j=1,\dots,n,$$

with $\nabla\hat{\lambda}_i(v_j)$ defined as in (31).

Proof. Without loss of generality, we only consider the case $j=1$, so that A_1, A_n, B_2, B_n, and r_1 converge to zero as v approaches v_1, while B_1 converges to $-C_1$ and all other A_i, B_i, and r_i converge to positive real numbers. We recall from the proof of Lemma 2 that the quotients A_1/r_1^p and A_n/r_1^p converge to zero and note that similar arguments can be used to show that

$$\lim_{v\to v_1}\frac{B_2(v)}{r_1(v)^p}=0,\qquad \lim_{v\to v_1}\frac{B_n(v)}{r_1(v)^p}=0. \tag{32}$$

We also remember from the proof of Lemma 3 that the quotients A_1/r_1 and A_n/r_1 are bounded for any $v\in\Omega_\epsilon$ and likewise for the quotients B_2/r_1 and B_n/r_1, so that

$$\lim_{v\to v_1}\frac{A_1(v)A_n(v)}{r_1(v)^{p+1}}=0,\qquad \lim_{v\to v_1}\frac{B_2(v)A_n(v)}{r_1(v)^{p+1}}=0,\qquad \lim_{v\to v_1}\frac{B_n(v)A_1(v)}{r_1(v)^{p+1}}=0. \tag{33}$$

We now apply the product rule to the right hand side of (10) to get

$$\nabla\hat{w}_i=\mathcal{R}_{i+1}\nabla\mathcal{A}_i+\mathcal{A}_i\nabla\mathcal{R}_{i+1}-\mathcal{R}_iB_i\nabla\mathcal{A}_{i-1,i}-\mathcal{R}_i\mathcal{A}_{i-1,i}\nabla B_i-\mathcal{A}_{i-1,i}B_i\nabla\mathcal{R}_i+\mathcal{A}_{i-1}\nabla\mathcal{R}_{i-1}+\mathcal{R}_{i-1}\nabla\mathcal{A}_{i-1},$$

and further expand this sum using

$$\nabla\mathcal{A}_k=\sum_{\substack{l=1\\ l\neq k}}^{n}\mathcal{A}_{k,l}\nabla A_l,\qquad \nabla\mathcal{R}_k=-p\mathcal{R}_k\sum_{\substack{l=1\\ l\neq k}}^{n}\frac{s_l}{r_l},$$

where $s_l(v)=(v-v_l)/r_l(v)$ is the unit vector pointing from v_l into the direction of v. A careful analysis then reveals that most of the terms converge to zero for $i\neq 1$, because they contain at least one factor (A_1, A_n, B_2, or B_n) that vanishes at v_1 or one of the quotients in (12), (13), (32), or (33) that converges to zero, while all other factors either converge to finite values or (in the case of s_1) are bounded as v approaches v_1. The only terms that do not converge to zero emerge from $\mathcal{R}_1\nabla\mathcal{A}_1$ in the case $i=2$ and from $\mathcal{R}_1\nabla\mathcal{A}_n$ in the case $i=n$, and overall we get

$$\lim_{v\to v_1}\nabla\hat{w}_i(v)=\begin{cases}\mathcal{R}_1(v_1)\mathcal{A}_{n,1}(v_1)\nabla A_n, & i=2,\\ 0, & i=3,\dots,n-1,\\ \mathcal{R}_1(v_1)\mathcal{A}_{n,1}(v_1)\nabla A_1, & i=n.\end{cases} \tag{34}$$

The remaining gradient $\nabla\hat{w}_1$ diverges at v_1, but it turns out that multiplying it with any of the $\hat{w}_i$, $i=2,\dots,n$, which converge to zero as v approaches v_1, as shown in the proofs of Lemmas 1 and 2, is sufficient to counterbalance the divergence. Indeed, it follows, using the same arguments as above, that

$$\lim_{v\to v_1} \hat{w}_i(v)\nabla\hat{w}_1(v) = 0, \qquad i=2,\dots,n. \tag{35}$$

By the chain rule, (34), (35), and the fact that $\hat{W}$ converges to $\mathcal{R}_1(v_1)C_1\mathcal{A}_{n,1}(v_1)$, we finally get

$$\lim_{v\to v_1} \nabla\hat{\lambda}_i(v) = \lim_{v\to v_1}\left(\frac{\nabla\hat{w}_i(v)}{\hat{W}(v)} - \frac{\hat{w}_i(v)\sum_{j=1}^n \nabla\hat{w}_j(v)}{\hat{W}(v)^2}\right) = \frac{1}{C_1}\begin{cases}\nabla A_n, & i=2,\\ 0, & i=3,\dots,n-1,\\ \nabla A_1, & i=n.\end{cases}$$

For $i=1$, we note that $\hat{\lambda}_1 = 1-\sum_{i=2}^n \hat{\lambda}_i$ and therefore

$$\lim_{v\to v_1} \nabla\hat{\lambda}_1(v) = -\lim_{v\to v_1}\sum_{i=2}^n \nabla\hat{\lambda}_i(v) = -\frac{\nabla A_n + \nabla A_1}{C_1} = \frac{-\nabla B_1}{C_1},$$

where the last step follows from the fact that $A_n + A_1 = B_1 + C_1$. □

Theorem 3. *For any $p<1$, there exists an $\epsilon>0$, such that the exponential three-point coordinates are continuously differentiable over Ω_ϵ.*

Proof. Theorem 2 guarantees the existence of an ϵ for any $p<1$, such that $\hat{\lambda}_i$ is well-defined and continuous over Ω_ϵ. It further follows from (10) that $\hat{\lambda}_i$ is infinitely differentiable over $\Omega_\epsilon \setminus \bigcup_{j=1}^n v_j$, because A_i, B_i, and r_i^{-p} are infinitely differentiable over this domain. Since the derivative of $\hat{\lambda}_i$ extends continuously to the v_j by Lemma 6, the differentiability at v_j follows by the multivariate mean value theorem. □

Remark 1. It has not escaped our notice that this result is somewhat little surprising for $p<0$. Clearly, if $p<-k$ for some $k\in\mathbb{N}_0$, then r_j^{-p} is C^k, and it follows from (10) that $\hat{\lambda}_i$, as a combination of these C^k functions and the C^∞ functions A_j and B_j, is C^k itself. Taking a closer look at (10), we further find that each r_j^{-p} can be paired with one of the linear functions A_{j-1}, A_j, B_{j-1}, or B_{j+1}, which vanish at v_j. Since these pairs are C^{k+1}, then so is $\hat{\lambda}_i$. Moreover, if $p=-2k$ for some $k\in\mathbb{N}$, then $\hat{\lambda}_i$ is a rational function, just as in the case of Wachspress coordinates ($p=0$), and likewise C^∞ over Ω_ϵ. However, the result is still quite remarkable for $0<p<1$, because both the numerator $\hat{w}_i$ and the denominator $\hat{W}$ are only C^0 at the vertices v_j in this case.

Figure 10 shows a close-up to an exponential three-point coordinate function in the region $\pm10^{-5}$ around the corresponding vertex. For $p\le 1/2$, the coordinate is visually identical to a linear function. As p increases, the slope of the function decreases inside and increases outside the polygon, but it remains C^1, as long as $p<1$. For $p=1$, the shape of the function is completely different, with a local, non-differentiable maximum at the vertex.

The proof of Lemma 6, and hence also Theorem 3, does not extend to the case $p\ge 1$, because the quotients in (33) diverge, and the following example shows that exponential three-point coordinates for $p\ge 1$ are, in general, not C^1 at the vertices of the polygon. As before, the polygon in the example was chosen to keep the formulas simple, but we observed the same phenomena for all other polygons that we tested.

Example 3. Let us consider the quadrilateral P with vertices $v_1=(1,0)$, $v_2=(0,1)$, $v_3=(-1/4,0)$, $v_4=(0,-1)$ and study the directional derivative of $\hat{\lambda}_3$ in direction $u=(1,0)$ at v_1 (see Figure 8, right). If $\hat{\lambda}_3$ were C^1 at v_1, then, according to (29) and (31), we would have $\nabla_u\hat{\lambda}_3(v_1)=0$. Instead, we get

$$\nabla_u\hat{\lambda}_3(v_1) = \lim_{h\to 0}\frac{\hat{\lambda}_3(1+h,0)}{h} = \frac{16\left(\frac{5\sqrt{2}}{8}\right)^p - 20}{25} < 0$$

for $p>1$, while for $p=1$ only the one-sided limits

$$\lim_{h\to 0^-}\frac{\hat{\lambda}_3(1+h,0)}{h} = \frac{8\sqrt{2}-12}{5} < 0 \qquad \text{and} \qquad \lim_{h\to 0^+}\frac{\hat{\lambda}_3(1+h,0)}{h} = -\frac{4}{5} < 0$$

exist.

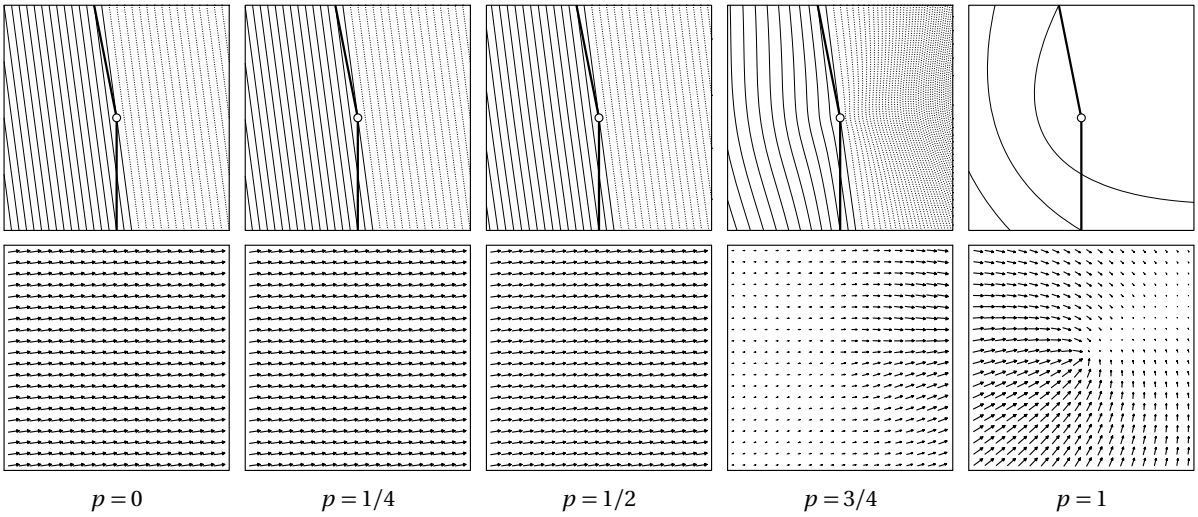

Figure 10: Contour plots (top) for contour values $\mathbb{Z} \cdot 10^{-5}$ and gradient vectors (bottom) of the exponential three-point coordinate corresponding to the middle right vertex of the convex polygon in Figure 9 (right) for different values of p (cf. Figure 2). Dotted lines indicate contour values greater than one.

3.1 Directional derivatives of mean value coordinates

It is clear that the directional derivatives of a C^1 function $f : \mathbb{R}^2 \to \mathbb{R}$ at $v \in \mathbb{R}^2$ in the unit directions $u \in S^1$ form a sinusoidal function with period 2π, because

$$\nabla_u f(v) = \nabla f(v) \cdot u = \|\nabla f(v)\| \cos\phi,$$

where ϕ is the angle between $\nabla f(v)$ and u. The plots in Figure 11 confirm that this is exactly how exponential three-point coordinates for $p < 1$ behave at the vertices. Instead, for mean value coordinates ($p = 1$), which are not C^1 at the vertices, the plots suggest that the one-sided directional derivatives also form a sinusoidal function with period 2π, but with non-zero vertical shift in this case.

To prove this interesting observation, we recall the definition of the one-sided directional derivative

$$\nabla_u^+ \lambda_i(v_j) = \lim_{h \to 0^+} \frac{\lambda_i(v_j + h\,u) - \lambda_i(v_j)}{h}$$

of λ_i at v_j in direction $u \in \mathbb{R}^2$ and define the normals

$$n_i = \frac{2v_i - v_{i-1} - v_{i+1}}{\|2v_i - v_{i-1} - v_{i+1}\|}, \qquad i = 1, \ldots, n,$$

that bisect the exterior angles at v_i.

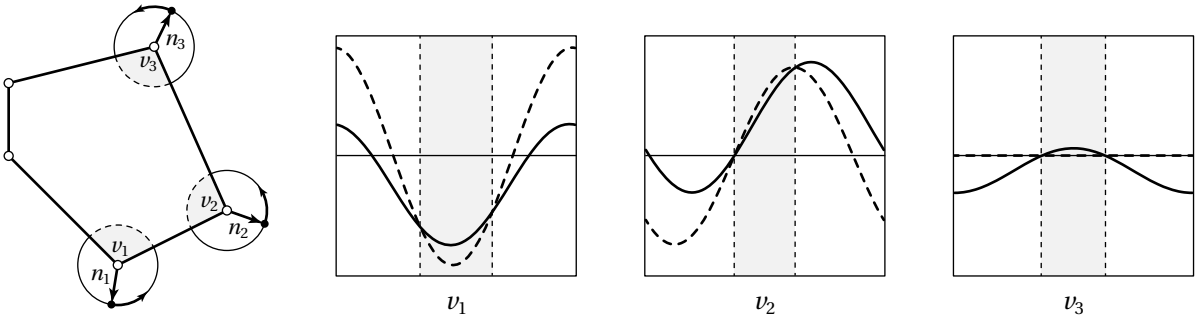

Figure 11: One-sided directional derivatives of λ_1 at v_1, v_2, and v_3 for $p < 1$ (dashed) and $p = 1$ (solid), parameterized by the signed angle to the normal n_1, n_2, and n_3, respectively. The grey area corresponds to the interval of the angle inside the polygon.

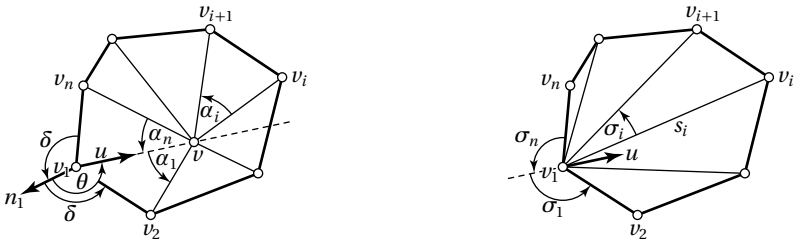

Figure 12: Notation used in the proof of Theorem 4.

Theorem 4. *The one-sided directional derivatives of mean value coordinates ($p=1$) at v_j in the unit directions $u \in S^1$ can be written as*

$$\nabla_u^+ \lambda_i(v_j) = a_{i,j}(\sin(\theta + \varphi_{i,j}) + b_{i,j}), \qquad i = 1,\dots,n, \quad j = 1,\dots,n,$$

where θ is the signed angle between n_i and u, and $a_{i,j}$, $b_{i,j}$, $\varphi_{i,j}$ are certain constants depending on P.

Proof. As shown in [3], mean value coordinates can also be defined by replacing the w_i in (2) with

$$w_i = \frac{\tan(\alpha_{i-1}/2) + \tan(\alpha_i/2)}{r_i}, \qquad i = 1,\dots,n$$

where α_i is the signed angle between $v_i - v$ and $v_{i+1} - v$ (see Figure 12). The advantage of this formula is that it can be used to evaluate the resulting coordinates λ_i everywhere, except at the boundary of the polygon, because the denominator W is non-zero for all $v \in \mathbb{R}^2 \setminus \partial\Omega$ [4].

Without loss of generality, we focus on the case $j = 1$ and consider the situation as v approaches v_1 along the ray defined by some unit vector $u \in S^1$ (see Figure 12). For the moment, we tacitly assume that u is not pointing along the adjacent edges E_1 and E_n, so that $w_i(v_1 + h\,u)$ is well-defined for sufficiently small $h > 0$. Denoting the signed angle between n_1 and u by θ, it is clear that α_1 and α_n converge to

$$\sigma_1 = \lim_{h\to 0^+} \alpha_1(v_1 + h\,u) = \delta + \pi - \theta \qquad \text{and} \qquad \sigma_n = \lim_{h\to 0^+} \alpha_n(v_1 + h\,u) = \delta + \theta - \pi,$$

where δ is the signed angle between n_1 and $v_2 - v_1$ and between $v_n - v$ and n_1 (see Figure 12). Letting $\sigma_i = \alpha_i(v_1)$, $i = 2,\dots,n-1$ and $s_i = r_i(v_1)$, $i = 2,\dots,n$, we have

$$\lim_{h\to 0^+} w_i(v_1 + h\,u) = \frac{\tan(\sigma_{i-1}/2) + \tan(\sigma_i/2)}{s_i}, \qquad i = 2,\dots,n.$$

Moreover, since $r_1(v_1 + h\,u) = h$,

$$\lim_{h\to 0^+} h\,w_i(v_1 + h\,u) = \begin{cases} \tan(\sigma_n/2) + \tan(\sigma_1/2), & i = 1, \\ 0, & i = 2,\dots,n. \end{cases}$$

For $i = 3,\dots,n-1$, we then get

$$\begin{aligned} \nabla_u^+ \lambda_i(v_1) = \lim_{h\to 0^+} \frac{w_i(v_1 + h\,u)}{h\,W(v_1 + h\,u)} &= \frac{\tan(\sigma_{i-1}/2) + \tan(\sigma_i/2)}{s_i} \cdot \frac{\cos(\sigma_n/2)\cos(\sigma_1/2)}{\sin((\sigma_n + \sigma_1)/2)} \\ &= \frac{\tan(\sigma_{i-1}/2) + \tan(\sigma_i/2)}{2 s_i \sin\delta} \big(\sin(\theta - \pi/2) + \sin(\delta + \pi/2)\big), \end{aligned}$$

and similarly, after some trigonometric simplifications,

$$\nabla_u^+ \lambda_2(v_1) = \frac{1}{2 s_2 \sin\delta \cos(\sigma_2/2)} \big(\sin(\theta - \sigma_2/2) + \sin(\delta + \sigma_2/2)\big)$$

and

$$\nabla_u^+ \lambda_n(v_1) = \frac{-1}{2 s_n \sin\delta \cos(\sigma_{n-1}/2)} \big(\sin(\theta + \sigma_{n-1}/2) - \sin(\delta + \sigma_{n-1}/2)\big).$$

If u is pointing along the adjacent edges E_1 or E_n, so that $\theta = \delta$ or $\theta = -\delta$, then these formulas give the correct values, and so they are valid for all $u \in S^1$. For the remaining case $i = 1$ we note that

$$\nabla_u^+ \lambda_1(v_1) = \lim_{h \to 0^+} \frac{w_1(v_1 + hu) - W(v_1 + hu)}{hW(v_1 + hu)} = \lim_{h \to 0^+} \sum_{i=2}^{n} \frac{-w_i(v_1 + hu)}{hW(v_1 + hu)} = -\sum_{i=2}^{n} \nabla_u^+ \lambda_i(v_1)$$

and that a sum of sinusoidal functions with period 2π is also a sinusoidal function with the same period. □

An immediate consequence of Theorem 4 is that the one-sided directional derivatives of mean value coordinates at the vertices are bounded. Further note that Theorem 4 also holds in the case of non-convex polygons, because the convexity of P is not used in the proof.

Remark 2. For $p > 1$, a similar analysis, based on the alternative representation of the coordinates λ_i using

$$w_i = \frac{1}{r_i} \left(\frac{r_{i-1}^{p-1} - r_i^{p-1} \cos \alpha_{i-1}}{\sin \alpha_{i-1}} + \frac{r_{i+1}^{p-1} - r_i^{p-1} \cos \alpha_i}{\sin \alpha_i} \right), \qquad i = 1, \ldots, n$$

instead of the w_i in (2), reveals that the one-sided directional derivatives of λ_i at v_j in the unit directions $u \in S^1$ can be written as

$$\nabla_u^+ \lambda_i(v_j) = a_{i,j} \frac{\sin(2\theta + \varphi_{i,j}) + b_{i,j}}{\sin(\theta + \psi_j)}, \qquad i = 1, \ldots, n, \quad j = 1, \ldots, n,$$

for certain constants $a_{i,j}$, $b_{i,j}$, $\varphi_{i,j}$, ψ_j depending on P. Note that the phase shift ψ_j in the denominator does not depend on i, and it can be shown that the common poles of all one-sided directional derivatives $\nabla_u^+ \lambda_i(v_j)$, $i = 1, \ldots, n$ at v_j occur in the directions $u = \pm t / \|t\|$, where

$$t = \big((v_{j+1} - v_j) \| v_{j-1} - v_j \|^p - (v_{j-1} - v_j) \| v_{j+1} - v_j \|^p \big),$$

and that t is tangent to the zero level curve $\{v \in \mathbb{R}^2 : \tilde{W}(v) = 0\}$. As both these directions clearly lie outside P, the one-sided directional derivatives are well-defined and bounded over $\bar{\Omega}$.

4 Conclusion

Based on the results above, we can split the family of exponential three-point coordinates for planar convex polygons into three sub-families with different behaviour: (1) for $p < 1$, which includes Wachspress coordinates ($p = 0$), these coordinates are well-defined and at least C^1 in an ϵ-neighbourhood of the polygon; (2) for $p > 1$, which includes discrete harmonic coordinates ($p = 2$), they are well-defined over the polygon, but not necessarily in its vicinity and only C^0 at the vertices of the polygon; (3) mean value coordinates ($p = 1$) are well-defined and C^∞ everywhere in the plane, except at the vertices, where they are C^0 with bounded directional derivatives.

Acknowledgements

We wish to thank Ulrich Reif for inspiring discussions and helpful comments. This work was supported by the Swiss National Science Foundation (SNSF) under project numbers 200020_156178 and P2TIP2_175859.

References

[1] M. Eck, T. DeRose, T. Duchamp, H. Hoppe, M. Lounsbery, and W. Stuetzle. Multiresolution analysis of arbitrary meshes. In *Proceedings of SIGGRAPH*, pages 173–182, Los Angeles, Aug. 1995.

[2] M. S. Floater. Mean value coordinates. *Computer Aided Geometric Design*, 20(1):19–27, Mar. 2003.

[3] M. S. Floater, K. Hormann, and G. Kós. A general construction of barycentric coordinates over convex polygons. *Advances in Computational Mathematics*, 24(1–4):311–331, Jan. 2006.

[4] K. Hormann and M. S. Floater. Mean value coordinates for arbitrary planar polygons. *ACM Transactions on Graphics*, 25(4):1424–1441, Oct. 2006.

[5] A. F. Möbius. *Der barycentrische Calcul.* Johann Ambrosius Barth Verlag, Leipzig, 1827.

[6] U. Pinkall and K. Polthier. Computing discrete minimal surfaces and their conjugates. *Experimental Mathematics*, 2(1):15–36, 1993.

[7] E. L. Wachspress. *A Rational Finite Element Basis*, volume 114 of *Mathematics in Science and Engineering*. Academic Press, New York, 1975.